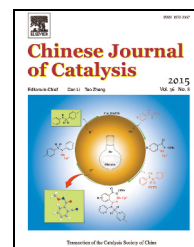


available at www.sciencedirect.comjournal homepage: www.elsevier.com/locate/chnjc

Article

Efficient solvent-free synthesis of pyridopyrazine and quinoxaline derivatives using copper-DiAmSar complex anchored on SBA-15 as a reusable catalyst

Marzieh Mohammadi^a, Ghasem Rezanejade Bardajee^{b,*}, Nader Noroozi Pesyan^a^a Department of Chemistry, Faculty of Science, Urmia University, 57159, Urmia, Iran^b Department of Chemistry, Payame Noor University, P.O. BOX, 19395-3697, Tehran, Iran

ARTICLE INFO

Article history:

Received 14 February 2015

Accepted 17 March 2015

Published 20 August 2015

Keywords:

DiAmSar

SBA-15

Heterogeneous catalyst

Pyridopyrazine

Quinoxaline

ABSTRACT

A catalytic system comprising mesoporous silica functionalized with Cu(II)-DiAmSar was synthesized. This was demonstrated as an efficient heterogeneous catalyst for the synthesis of biologically useful pyridopyrazine and quinoxaline heterocycles under solvent-free conditions. X-ray diffraction, transmission electron microscopy, N₂ adsorption-desorption, Fourier transformation infrared spectroscopy, and thermogravimetric analysis were used to characterize the catalyst and investigate the texture of SBA-15 during the grafting process.

© 2015, Dalian Institute of Chemical Physics, Chinese Academy of Sciences.

Published by Elsevier B.V. All rights reserved.

1. Introduction

Natural and synthetic quinoxalines and their derivatives are well-known for their biological activities, including antiviral, antibacterial, anti-inflammatory, antiprotozoal, and kinase inhibitor behavior [1,2]. There are many pharmaceutical drugs such as Varenicline **1** (aid in smoking cessation), Brimonidine **2** (antiglaucoma activity), and Quinacillin **3** (antibacterial properties) that contain quinoxaline cores (Fig. 1) [3–5]. Thus, there is still a need for the development of a new, convenient, and environmentally benign synthesis approach.

In recent years, the heterogenization of homogeneous catalysts has attracted attention because this overcomes several disadvantages such as tedious purification of the product and undesired wastewater produced in homogeneous base-catalyzed processes. Furthermore, many homogeneous

systems consist of a metal and ligands in a particular stoichiometric ratio, and the removal of the ligands makes the purification of the product even more expensive. The design and development of new types of heterogeneous catalysts can mitigate these problems as it allows the straightforward removal of the catalyst from the reaction system.

Mesoporous silica has recently gained considerable attention in organic synthesis under heterogeneous reaction conditions, but they are not often used as catalysts. The surface functionalization of mesoporous silica by grafting or co-condensation is a promising approach for preparing efficient solid base catalysts. This method provides a way to attach catalytic centers onto mesoporous silica and avoids metal ion leaching [6–10]. Various silica supports like the M41S materials and SBA families with pore sizes between 2 and 50 nm have received attention in catalysis due to their high surface area (up

* Corresponding author. Tel: +98-28-33336366; Fax: +98-28-33344081; E-mail: rezanejad@pnu.ac.ir

This work was supported by Payame Noor University.

DOI: 10.1016/S1872-2067(15)60845-2 | <http://www.sciencedirect.com/science/journal/18722067> | Chin. J. Catal., Vol. 36, No. 8, August 2015

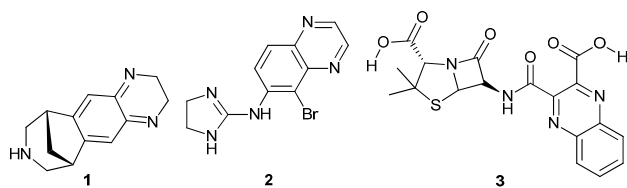
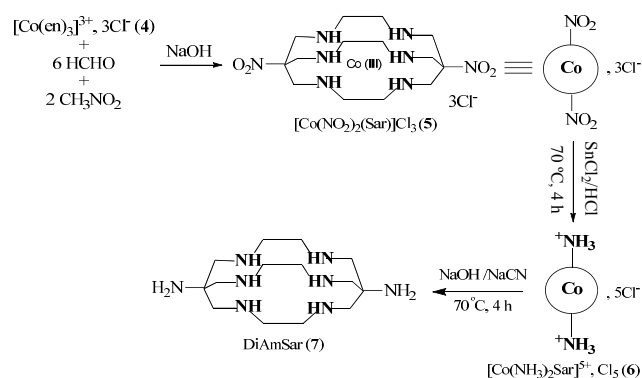


Fig. 1. Drug products that contain quinoxaline cores.

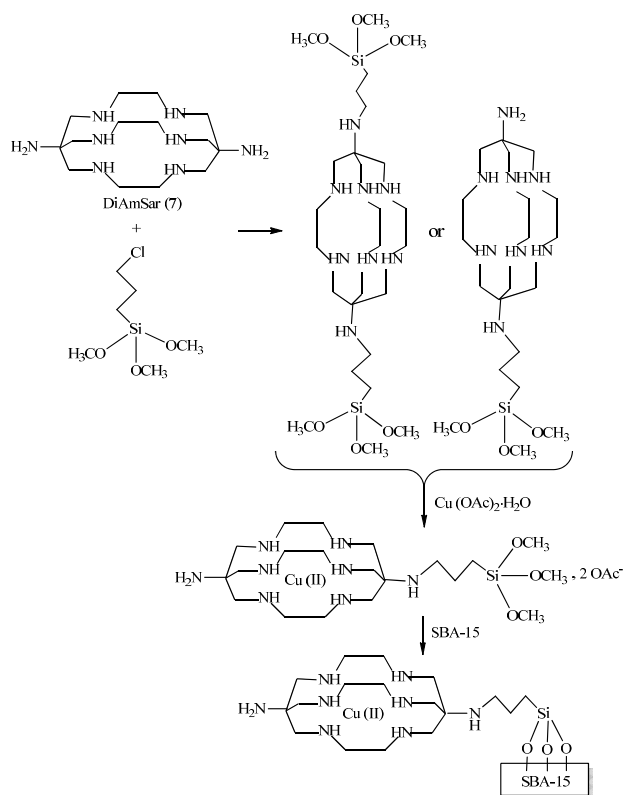
to 1200 m²/g), uniform and tunable pore size, organic solvent tolerance, and large diversity in surface functionalization [11–13]. SBA-15 is the most well-known representative of this class of materials with good hydrothermal stability, hexagonal arrays of uniform pores with a high specific surface area, sufficient silanol groups for surface modification, and large pore volume that facilitates the grafting of homogeneous metal compounds through coordinative linkage [14–16].

Nowadays, organic-inorganic hybrids are of great interest because they combine the advantages of heterogeneous catalysts (high mechanical, thermal, and structural stability) and organic molecules (flexibility and functionality) [17,18]. We have focused on the synthesis of some heterogeneous organometallic catalysts and applied them in organic synthesis [19–23]. Here we report the application of a novel heterogeneous catalyst for the synthesis of biologically active pyrido[2,3-*b*]pyrazine and quinoxaline heterocycles under solvent-free conditions. The procedure for the preparation of the heterogeneous nanocatalyst is described in Schemes 1 and 2 [24]. The catalyst consists of DiAmSar ligands **7** (hexaminemacrobicyclic cage amine ligands which are known by their trivial name, sarcophagines, Scheme 1). This not only forms remarkably stable complexes with transition metal ions such as Cu(II), but also have fast complexation kinetics even at a low concentration of metal ions [25,26]. So this catalytic system has virtually no Cu-leaching. DiAmSar-based ligands are also appropriate for the encapsulation of radioisotope metal ions. They can conjugate to peptides, antibodies, and biologically compatible polymers by their amine functional groups, so they can be radio-labelled with PET (diagnostic positron emission tomography) isotopes for the imaging of molecular interactions [27–30].

To prepare the title heterogeneous catalyst, Cu(II)-DiAmSar complex was anchored onto the SBA-15 mesoporous material.



Scheme 1. Preparation of DiAmSar.



Scheme 2. Preparation of Cu(II)-DiAmSar complex anchored on SBA-15 (Cu(II)-DiAmSar/SBA-15).

(3-Chloropropyl)trimethoxysilane reacted with the DiAmSar's amine functionality, complexed with the Cu(II) salt and was covalently immobilized on SBA-15 through the trimethoxysilane moiety (Scheme 2).

2. Experimental

2.1. Materials

Acetonitrile, ethanol, formaldehyde, NaOH, methanol, stannous chloride dihydrate, CoCl₂·6H₂O, sodium cyanide, nitromethane, ethylenediamine, commercial 1,2-phenylenediamines, 2,3-diaminopyridine, 3,4-diaminopyridine, 1,2-dicarbonyl compounds, poly(ethylene oxide)-block-poly(propylene oxide)-block-poly(ethylene oxide) triblock copolymer (P123), (3-chloropropyl)trimethoxysilane (CPTMS), copper (II) acetate monohydrate, tetraethyl orthosilicate (TEOS), HNO₃, and HCl were purchased from Sigma-Aldrich, Merck, and Acros chemical companies. Doubly distilled water was used when necessary. All materials were used without further purification. The solvents used for the synthesis were analytical grade and were used as received. Silica gel (Merck, grade 9385, 230–400 mesh, 60 Å) for column chromatography was used as received. All other reagents were purchased from Merck and used as received unless otherwise noted. The course of the synthesis of the heterocycle was followed by TLC on a silica gel plate (Merck, silica gel 60 F₂₅₄, ready-use) using methanol (9:1) or *n*-hexane:ethyl acetate (1:3) as eluent. The eluent for column chromatography was the same as the TLC eluent.

2.2. Characterization

Transmission electron microscopy (TEM) observation was performed with a Hitachi H-700 CTEM. Fourier transformation infrared (FT-IR) spectra were recorded using KBr pellets on a Jasco 4200 FT-IR spectrophotometer. X-ray diffraction (XRD; Bruker D8ADVANCE with Ni-filtered Cu $K\alpha$ radiation at 1.5406 Å) was carried out with a speed of 2°/min and a step of 0.05°. ^1H and ^{13}C NMR spectra were recorded at room temperature on Bruker AC 300 and 500 MHz spectrometers using CDCl_3 or DMSO-d_6 as the NMR solvent. ^1H NMR spectra were referenced to tetramethylsilane (0.00 ppm), and ^{13}C NMR spectra were referenced from the solvent central peak (for example, 77.23 ppm for CDCl_3). Chemical shifts are given in ppm. N_2 adsorption-desorption isotherms were obtained at $-196\text{ }^\circ\text{C}$ with a Quantachrome Autosorb-1 apparatus. Before measurement, the sample was outgassed at $120\text{ }^\circ\text{C}$ for 12 h. The specific surface area and pore size distribution were obtained from the desorption branch of the isotherm using the BET method and BJH analysis, respectively. A Shimadzu AA-6300 flame atomic absorption spectrometer was used to get the concentration of metal ions. For this purpose, 0.1 g of the catalyst was digested by HNO_3 with stirring at room temperature for a week. Then the mixture was filtered and the solid was washed several times with water to get a colourless filtrate solution for metal measurement. The concentration of Cu(II) in the immobilized SBA-15 was 0.016 mmol/g. Thermogravimetric analysis (TGA) was carried out with a TGA/DTA Shimadzu-50 instrument equipped with a platinum pan. The sample was heated in air from 25 to $1000\text{ }^\circ\text{C}$ with a heating rate of $10\text{ }^\circ\text{C}/\text{min}$. The weight loss was recorded as a function of temperature. Melting points were recorded using a Buchi B540 melting point apparatus and were uncorrected.

2.3. General procedure for the synthesis of pyrazine-based heterocycles under solvent-free conditions

A round-bottomed flask equipped with a magnet and condenser was charged with the desired 1,2-diamine (1.0 mmol), 1,2-diketone (1.0 mmol), and catalyst (Cu(II)DiAmSar/SBA-15, 0.005 g). The resulting mixture was heated at $100\text{ }^\circ\text{C}$ for the appropriate time. The course of the reaction was monitored using TLC on silica gel. Finally, the reaction mixture was cooled, and the crude mixture was purified by column chromatography or crystallization to get the desired product. Spectral and physical data for all heterocycles were compared with reference samples and were in accord with previously reported data.

Selected spectroscopic data for compounds **10v** and **10w** were as follows.

8-Methyl-8,9-dihydro-acenaphtho[1,2-b]pyrazine 10v. Yield 98%; yellow solid, mp: $73\text{--}75\text{ }^\circ\text{C}$. IR (KBr) ν (cm^{-1}): 3010, 2929, 1680, 1492, 1121. ^1H NMR (300 MHz, CDCl_3) δ 1.45 (d, $J = 7.1$ Hz, 3H), 3.54 (dd, $J = 11.1$ Hz, 6.0 Hz, 1H), 3.84–3.92 (m, 1H), 4.06 (dd, $J = 10.9$ Hz, 6.1 Hz, 1H), 7.65 (t, $J = 7.5$ Hz, 2H), 7.89–7.95 (m, 4H). ^{13}C NMR (75 MHz, CDCl_3) δ 158.3, 157.9, 141.6, 131.7, 131.5, 130.6, 128.4, 128.2, 127.8, 118.7, 118.6, 51.8, 49.7, 20.2. Anal. Calcd. for $\text{C}_{15}\text{H}_{12}\text{N}_2$ (220.2): C, 81.79; H, 5.49; N, 12.72. Found: C, 81.68; H, 5.35; N, 12.59.

2-Methyl-dibenzo[f,h]quinoxaline 10w. Yield 80%; white solid, mp: $121\text{--}123\text{ }^\circ\text{C}$. IR (KBr) ν (cm^{-1}): 3018, 2920, 1610, 1501, 1212. ^1H NMR (300 MHz, CDCl_3) δ 2.84 (s, 1H), 7.71–7.80 (m, 4H), 8.62 (d, $J = 7.5$ Hz, 2H), 8.77 (s, 1H), 9.18 (d, $J = 8.1$ Hz, 1H), 9.26 (d, $J = 7.5$ Hz, 1H). ^{13}C NMR (75 MHz, CDCl_3) δ : 152.6, 143.8, 140.2, 138.7, 131.4, 130.9, 130.0, 129.9, 129.2, 128.9, 128.4, 127.6, 127.5, 125.3, 124.9, 122.6, 22.2. Anal. Calcd. for $\text{C}_{17}\text{H}_{12}\text{N}_2$ (244.2): C, 83.58; H, 4.95; N, 11.47. Found: C, 83.65; H, 4.82; N, 11.30.

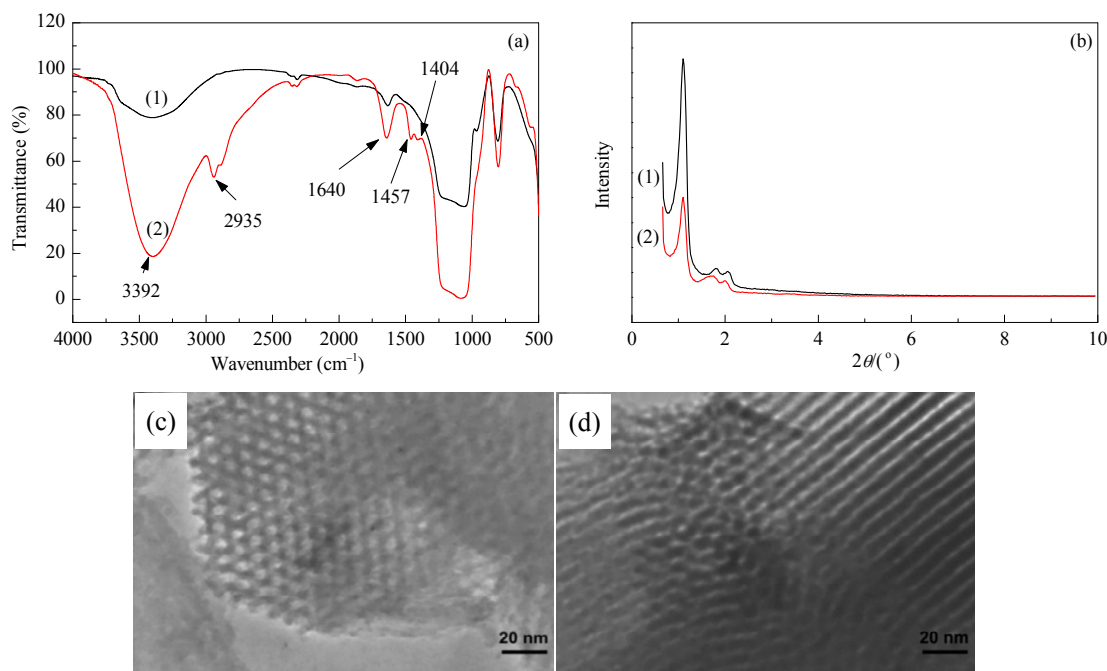


Fig. 2. (a) FT-IR spectra of SBA-15 (1) and Cu(II)-DiAmSar/SBA-15 (2). (b) XRD patterns of SBA-15 (1) and Cu(II)-DiAmSar/SBA-15(2). (c,d) TEM images of Cu(II)-DiAmSar/SBA-15. (c) in the direction of the pore axis; (d) in the perpendicular direction to the pore axis.

3. Results and discussion

3.1. Characterization of Cu(II)-DiAmSar complex anchored onto SBA-15

The successful grafting of the Cu(II)-DiAmSar complex onto SBA-15 was characterized using various physico-chemical techniques. The FT-IR spectra of SBA-15 and Cu(II)-DiAmSar/SBA-15 are shown in Fig. 2(a). Cu(II)-DiAmSar/SBA-15 showed both the silica framework and DiAmSar complex characteristic bands, including a strong absorbing band at 1000–1200 cm^{-1} (stretching vibration of the Si–O–Si bond), a broad band between 3000 and 3600 cm^{-1} (stretching vibration of NH (from DiAmSar) and OH (from SBA-15) groups), a peak at 1640 cm^{-1} (bending of the NH group), a medium band observed at 2955 cm^{-1} (stretching vibration of CH_2), and peaks at 1400–1500 cm^{-1} (absorption peaks of C–N groups).

The quality and structural ordering of Cu(II)-DiAmSar/SBA-15 were determined by XRD. The XRD patterns of both SBA-15 and Cu(II)-DiAmSar/SBA-15 (Fig. 2(b)) exhibited an intense peak at 1.1° corresponding to the (100) reflection, and two low intensity peaks at 1.72° and 1.98° that were indexed as the (110) and (200) reflections. These peaks are from the ordered hexagonal unit cell of the mesoporous material and showed that the structure of mesoporous SBA-15 was retained during immobilization [31]. Furthermore, the lower angle in the XRD pattern of Cu(II)-DiAmSar/SBA-15 was due to the development of a unit cell arising from the connection of the complex in SBA-15, and the lower intensity was due to a decrease in the mesoscopic order.

The TEM images of Cu(II)-DiAmSar/SBA-15 are presented in Fig. 2(c) and (d) in the direction of the pore axis (Fig. 2(c)) and perpendicular to the pore axis of Cu(II)-DiAmSar/SBA-15 (Fig. 2(d)). The TEM images of the supported complex confirmed the retaining of the cylindrical shape of the pores and the hexagonal arrays of uniform channels.

N_2 adsorption-desorption isotherms and pore size distributions of the samples are depicted in Fig. 3(a). Both SBA-15 and Cu(II)-DiAmSar/SBA-15 exhibited type IV isotherms with a small H_1 hysteresis loop, showing that the

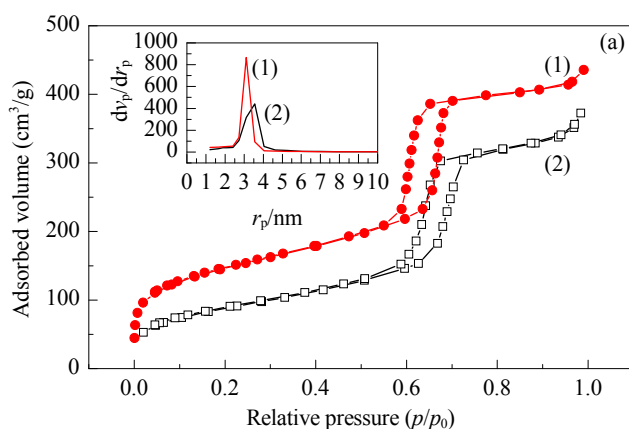


Table 1

Textural properties of SBA-15 and Cu(II)-DiAmSar/SBA-15.

Material	$S_{\text{BET}}^{\text{a}}$ (m^2/g)	$V_{\text{BjH}}^{\text{b}}$ (cm^3/g)	$D_{\text{BjH}}^{\text{c}}$ (nm)
SBA-15	532	0.600	6.24
Cu(II)-DiAmSar/SBA-15	317	0.560	6.10

^aSpecific surface area.

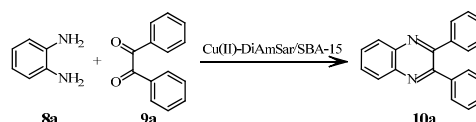
^bPore volume.

^cPore diameter (calculated from the adsorption branch).

cage-like structure of SBA-15 was maintained after grafting with Cu(II)-DiAmSar [32]. The textural parameters of the samples are collected in Table 1. As can be seen, the surface area, pore diameter, and pore volume of Cu(II)-DiAmSar/SBA-15 decreased with the immobilization of Cu(II)-DiAmSar inside the channels of SBA-15.

Table 2

Screening of the reaction conditions for the reaction of 1,2-phenylenediamine **8a** and benzil **9a**.



Entry	Solvent	Catalyst (10^{-5} mmol)	$t/^\circ\text{C}$	Time (min)	Yield ^a (%)
1	Free	0	rt	320	—
2	Free	8	rt	10	30
3	Free	16	rt	10	30
4	Free	0.8	rt	10	20
5	Free	8	60	10	65
6 ^b	Free	8	100	10	99 (98 ^c)
7	H_2O	8	Reflux	120	80
8	EtOH	8	Reflux	100	85
9	DMF	8	100	80	78
10	Toluene	8	Reflux	160	85

Reaction conditions: 1,2-Phenylenediamine **8a** (1 mmol, 1 equiv), benzil **9a** (1.0 mmol, 1 equiv) and catalyst (0–0.00016 mmol based on Cu(II) ions or 0–0.05 g of Cu(II)-DiAmSar/SBA-15) were heated for an appropriate time in a solvent (2 mL) or solvent-free conditions.

^aBased on GC yields.

^bOptimum conditions.

^cIsolated yield.

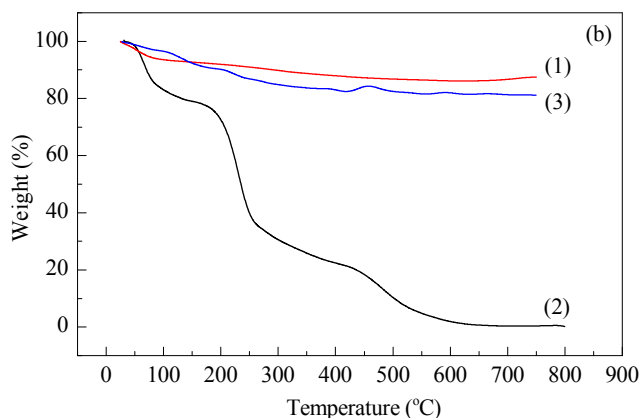


Fig. 3. (a) N_2 adsorption isotherms and corresponding pore size distributions (inset) of SBA-15 (1) and Cu(II)-DiAmSar/SBA-15(2). (b) TGA curves of SBA-15(1), Cu(II)-DiAmSar/SBA-15(2), and DiAmSar (3).

Figure 3(b) illustrates the TGA profiles of pure SBA-15 and Cu(II)-DiAmSar/SBA-15. Pure siliceous SBA-15 showed a mass loss below 100 °C due to the loss of physically adsorbed water from the surface of SBA-15. The thermogram of Cu(II)-DiAmSar/SBA-15 showed weight losses at two temperatures: the weight loss at 100 °C was from dehydration and the weight loss between 200 and 700 °C was from the thermal decomposition of grafted Cu(II)-DiAmSar moieties. These results confirmed the successful grafting of the Cu(II)-DiAmSar complex on the SBA-15 surface. According to the TGA data, the grafting amount

of DiAmSar on SBA-15 was 62 wt% (based on the initial amount of DiAmSar used for the anchoring).

3.2. Catalyst activity

To test the activity of the catalyst, initially, the reaction between 1,2-phenylenediamine (**8a**) and benzil (**9a**) was selected as a model reaction to find the best reaction conditions (Table 2). In the first attempt, we examined the reaction at room temperature in the absence of the catalyst, which gave no

Table 3
Synthesis of 2,3-disubstituted quinoxalines catalyzed by Cu(II)-DiAmSar/SBA-15.

Entry	Diamine 8	Diketone 9	Product 10	Yield (%)	Time (min)	m.p. (°C) (lit.)
1				98	10	121–123 (124 [33])
2	8a			92	10	148–150 (151–152.5 [33])
3	8a			99	5	133–134 (135–137 [33])
4	8a			99	5	102–104 (104–106 [34])
5		9a		88	30	183–185 (183 [34])
6	8b	9d		99	5	130–132 (131–133 [35])
7		9a		99	5	114–116 (110–111 [35])
8	8c	9b		96	20	123–125 (124–126 [35])
9	8c	9d		99	5	90–92 (92–94 [35])

Reaction conditions: 1,2-Phenylenediamine **8a** (1 mmol, 1 equiv), benzil **9a** (1.0 mmol, 1 equiv) and catalyst (0.005 g of Cu(II)-DiAmSar/SBA-15 or 8×10^{-5} mmol based on Cu(II) ions) were heated at 100 °C under solvent-free conditions.

yield of product. Although using dimethylformamide and ethanol as solvent gave reasonable yields (Table 2, entries 8 and 9), the best yield was obtained under the solvent-free condition at 100 °C and in the presence of 8×10^{-5} mmol of the catalyst (Table 2, entry 6).

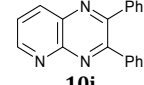
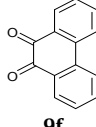
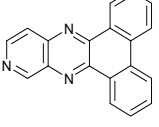
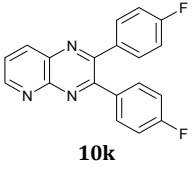
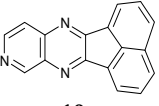
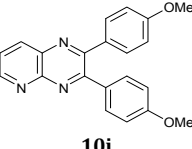
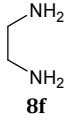
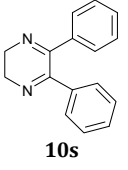
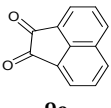
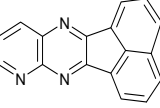
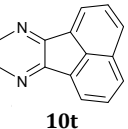
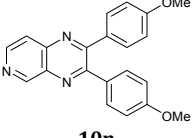
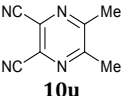
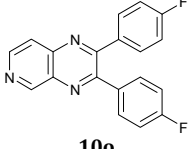
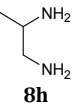
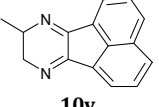
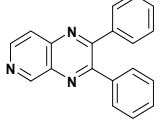
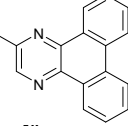
With the optimized conditions in hand, the generality of the reaction was evaluated by using various diamines and 1,2-diketones (Tables 3 and 4). Most of the substrates gave good to excellent yields in short reaction times.

The reactivity of aromatic and hetero-aromatic diamines is generally dominated by electronic effects. In general, aromatic and hetero-aromatic diamines with electron-withdrawing groups (EWG) react more slowly when compared to other diamines. For example, the condensation reaction of less electron-rich diamines, including substituted 1,2-

phenylenediamines bearing EWG (Table 3, entry 5) and diaminopyridines (Table 4, entries 1–9), was slower and gave lower yields. The reactivity of the aliphatic diamines with various 1,2-diketones was good (Table 4, entries 10–12 and 14). New quinoxaline derivatives were synthesized through the reactions of aliphatic diamine (1,2-diaminopropane **8h**) with acenaphthenequinone **9e** and phenanthrenequinone **9f** (Table 4, entries 13 and 14) in high yields and at lower temperature than the optimized conditions. The initial products of the aliphatic diamines can undergo a further oxidation step to give fully aromatic and stable final products (Table 4, entries 10, 11, and 13). For example, the reaction of aliphatic diamine **8h** and diketone **9f** (Table 4, entry 14) gave directly the final product **10w** (fully aromatic) via a one-pot protocol. The presence of a singlet peak at 2.84 ppm for the CH₃ group and another singlet

Table 4

Synthesis of pyridopyrazine and pyrazine derivatives in the presence of a catalytic amount of Cu(II)-DiAmSar/SBA-15.

En-try	Diamine 8	Diketone 9	Product 10	Yield (%)	Time (min)	m.p. (°C) (lit.)	En-try	Diamine 8	Diketone 9	Product 10	Yield (%)	Time (min)	m.p. (°C) (lit.)
1		9a		80	45	141–143 (142–143 [35])	8	8e			80	50	217–218 (216–218 [20])
2	8d	9c		85	45	142–144 (140–142 [20])	9	8e	9e		80	50	246–248 (245–247 [20])
3	8d	9b		77	90	137–139 (139–140 [35])	10		9a		99	5	154–156 (160–161 [34])
4	8d			88	60	222–224 (225–227 [20])	11	8f	9e		99	5	162–164 (165–167 [20])
5		9b		74	90	145–147 (147–148 [37])	12		9d		95	5	160–162 (162–164 [20])
6	8e	9c		78	50	133–135 (132–134 [20])	13		9e		98	5	73–75
7	8e	9a		79	60	170–172 (173–174 [36])	14	8h	9f		81	5	121–123

Reaction conditions: 1,2-Phenylenediamine **8a** (1 mmol, 1 equiv), benzil **9a** (1.0 mmol, 1 equiv) and catalyst (0.005 g of Cu(II)-DiAmSar/SBA-15 or 8×10^{-5} mmol based on Cu(II) ions) were heated at 100 °C under solvent-free conditions.

peak at 8.77 ppm for the CH group (in pyrazine ring, compound **10w**) in the ^1H NMR spectrum demonstrated the synthesis of this derivative. To get more details about the intermediate, we investigated the corresponding reaction for compound **10w** (unoxidized compound). The reaction was quenched at half its completion time, and the ^1H NMR of the crude mixture was analyzed (Fig. 4).

The appearance of a doublet peak at 1.46 ppm for CH_3 (peak b) and CH_2 diastereotopic hydrogen peaks (d and e peaks) at 3.31 and 3.99 ppm (Fig. 4, compound **10x**) demonstrated the presence of an unoxidized intermediate (compound **10x**) in the reaction mixture. Although products obtained from aliphatic diamines can be fully aromatic compounds, this was not a general rule in our protocol. For instance, compound **10v** (Table 4, entry 13) was not oxidized during the reaction. This was demonstrated by the presence of the doublet peaks of CH_2 (diastereotopic hydrogen) at 3.54 and 4.05 ppm, multiplet peaks of CH hydrogen atom (the H on the carbon chiral center) at 3.88 ppm, and doublet peaks of the CH_3 hydrogen group at 1.46 ppm in ^1H NMR spectrum (compound **10v**).

Some of the reactions in Table 3 were fast enough that they were completed in shorter reaction times than that of the optimized conditions. Furthermore, the reactivity of 1,2-diketones with electron-donating groups was slower with different diamines, for both the time and yield of the reactions (Table 4, entries 3 and 5).

The reusability of the catalyst was examined by repeating the model reaction (compound **10a**) under the optimized conditions. After the first reaction with 98% yield, the catalyst

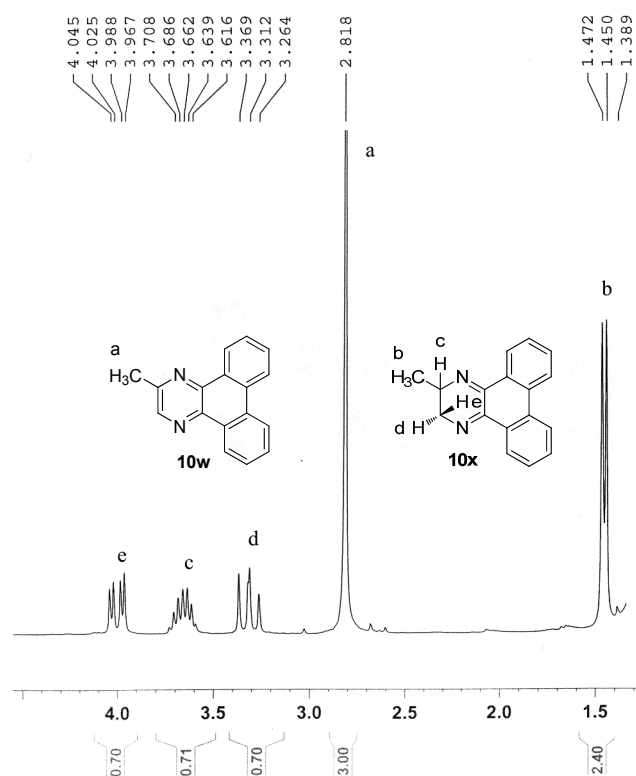


Fig. 4. ^1H NMR spectrum of a sample from the crude reaction mixture giving compound **10w**.

Table 5

Reuse of the catalyst for the synthesis of 2,3-diphenylquinoxaline **10a**.

Run	1	2	3	4	5	6	7
Isolated yield (%)	99	99	99	98	97	97	96

Table 6

Comparison of our results with some previously reported data for the synthesis of compound **10a**.

Method	Solvent	$t/^\circ\text{C}$	Time (min)	Yield (%)	Ref.
Zr(DS) ₄	H ₂ O	rt	30	94	[37]
MnCl ₂	EtOH	rt	17	94	[38]
Pd(II)-Schiff base/SBA-15	H ₂ O	100	30	99	[20]
—	HFIP	rt	60	95	[39]
Mont K-10 (10 mol%)	H ₂ O	rt	150	100	[40]
Silica sulfuric acid	EtOH	rt	15	98	[41]
Sulfamic acid	MeOH	25	5	100	[42]
In (5 nmol)/InCl ₃	MeOH	Reflux	30	85	[43]
Fe(III)-Schiff base/SBA-15	Water	Reflux	120	99	[22]
Cu(II)-DiAmSar/SBA-15	Solvent-free	100	5	99	This work

was first filtered, then washed with hot ethanol, and dried at 80 $^\circ\text{C}$ for 60 min. The recovered catalyst was used in another reaction, and we found that the Cu(II)-DiAmSar/SBA-15 catalyst can be recycled up to six times without any loss of activity (Table 5).

We compared some previously reported data for the synthesis of **10a** (Table 3, entry 1) with our protocol (Table 6). Our results were good in comparison to previously reported data in terms of yields, environment, and reaction times.

4. Conclusions

We synthesized and characterized a new active heterogeneous mesoporous catalyst of Cu(II)-DiAmSar complex grafted onto SBA-15. The catalyst was active for the synthesis of nitrogen containing pyrazine-based heterocycles, including pyrazine, pyrido[2,3-*b*]pyrazine, and quinoxaline derivatives, with good to excellent yields under mild conditions.

References

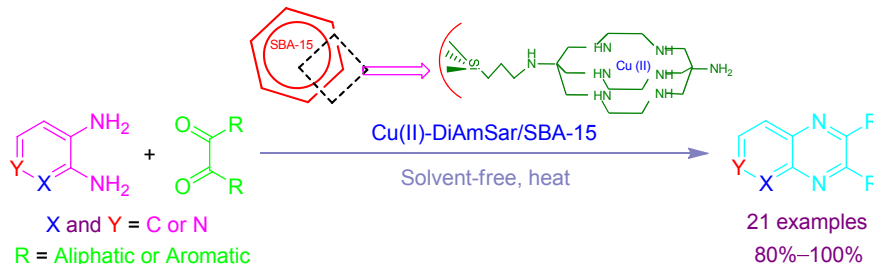
- [1] Yadav J S, Reddy B V S, Premalatha K, Shankar K S. *Synthesis*, 2008; 3787
- [2] He W, Myers M R, Hanney B, Spada A P, Bilder G, Galzcinski H, Amin D, Needle S, Page K, Jayyosi Z, Perrone M H. *Bioorg Med Chem Lett*, 2003, 13: 3097
- [3] Escobar-Chavez J J, Merino V, Lopez-Cervantes M, Rodriguez-Cruz I M, Quintanar-Guerrero D, Ganem-Quintanar A. *Curr Drug Discov Technol*, 2009, 6: 171
- [4] McLaughlin M A, Chiou G C Y. *J Ocul Pharmacol*, 1985, 1: 101
- [5] Hugo W B, Stretton R G. *Nature*, 1964, 202: 1217
- [6] Wu S H, Mou C Y, Lin H P. *Chem Soc Rev*, 2013, 42: 3862
- [7] Conley M P, Copéret C, Thieuleux C. *ACS Catal*, 2014, 4: 1458
- [8] Xie W L, Qi C. *J Agr Food Chem*, 2014, 62: 3348
- [9] Xie W L, Hu L B, Yang X L. *Ind Eng Chem Res*, 2015, 54: 1505
- [10] Xie W L, Zhao L L. *Energy Convers Manage*, 2014, 79: 34
- [11] Meynen V, Cool P, Vansant E F. *Microporous Mesoporous Mater*, 2009, 125: 170

Graphical Abstract

Chin. J. Catal., 2015, 36: 1379–1386 doi: 10.1016/S1872-2067(15)60845-2

Efficient solvent-free synthesis of pyridopyrazine and quinoxaline derivatives using copper-DiAmSar complex anchored on SBA-15 as a reusable catalyst

Marzieh Mohammadi, Ghasem Rezanejade Bardajee*, Nader Noroozi Pesyan
Urmia University, Iran; Payame Noor University, Iran



A silica-based mesoporous organic–inorganic hybrid catalyst was synthesized by anchoring Cu(II)-DiAmSar on SBA-15, which gave high activity for the synthesis of pyridopyrazine and quinoxaline derivatives under solvent-free conditions.

- [12] Liu J, Liu Y, Yang W, Guo H, Zhang H Z, Tang Z H, Fang F. *Mater Lett*, 2014, 128: 15
- [13] Shakeri M, Gebbink R J M K, de Jongh P E, de Jong K P. *Microporous Mesoporous Mater*, 2013, 170: 340
- [14] Walcarius A, Mercier L. *J Mater Chem*, 2010, 20: 4478
- [15] Yang Y, Zhang Y, Hao S J, Kan Q B. *Chem Eng J*, 2011, 171: 1356
- [16] Coperet C, Chabanas M, Saint-Arroman R P, Basset J M. *Angew Chem Int Ed*, 2003, 42: 156
- [17] Zou X C, Shi K Y, Wang C. *Chin J Catal*, 2014, 35: 1446
- [18] Zhu X C, Shen R W, Zhang L X. *Chin J Catal*, 2014, 35: 1716
- [19] Malakooti R, Bardajee G R, Hadizadeh S, Atashin H, Khanjari H. *Transit Metal Chem*, 2014, 39: 47
- [20] Motamedi R, Bardajee G R, Shakeri S. *Heterocycl Commun*, 2014, 20: 181
- [21] Malakooti R, Bardajee G R, Mahmoudi H, Kakavand N. *Catal Lett*, 2013, 143: 853
- [22] Bardajee G R, Malakooti R, Abtin I, Atashin H. *Microporous Mesoporous Mater*, 2013, 169: 67
- [23] Bardajee G R, Malakooti R, Jami F, Parsaei Z, Atashin H. *Catal Commun*, 2012, 27: 49
- [24] Mohammadi M, Bardajee G R, Pesyan N N. *RSC Adv*, 2014, 4: 62888
- [25] Qin C J, James L, Chartres J D, Alcock L J, Davis K J, Willis A C, Sargeson A M, Bernhardt P V, Ralph S F. *Inorg Chem*, 2011, 50: 9131
- [26] Geue R J, Hambley T W, Harrowfield J M, Sargeson A M, Snow M R. *J Am Chem Soc*, 1984, 106: 5478
- [27] Di Bartolo N, Sargeson A M, Smith S V. *Org Biomol Chem*, 2006, 4: 3350
- [28] Bell C A, Bernhardt P V, Gahan L R, Martinez M, Monteiro M J, Rodriguez C, Sharrad C A. *Chem Eur J*, 2010, 16: 3166
- [29] Cai H, Fissekis J, Conti P S. *Dalton Trans*, 2009: 5395
- [30] Hilderbrand S A, Weissleder R. *Curr Opin Chem Biol*, 2010, 14: 71
- [31] Pathak K, Ahmad I, Abdi S H R, Kureshy R I, Khan N H, Jasra R V. *J Mol Catal A*, 2008, 280: 106
- [32] Zhao D Y, Huo Q S, Feng J L, Chmelka B F, Stucky G D. *J Am Chem Soc*, 1998, 120: 6024
- [33] Heravi M M, Tehrani M H, Bakhtiari K, Oskooie H A. *Catal Commun*, 2007, 8: 1341
- [34] Darabi H R, Mohandessi S, Aghapoor K, Mohsenzadeh F. *Catal Commun*, 2007, 8: 389
- [35] Aghapoor K, Darabi H R, Mohsenzadeh F, Balavar Y, Daneshyar H. *Transit Metal Chem*, 2010, 35: 49
- [36] Antoine M, Czech M, Gerlach M, Günther E, Schuster T, Marchand P. *Synthesis*, 2011: 794
- [37] Hasaninejad A, Zare A, Zolfigol M A, Shekouhy M. *Synthetic Commun*, 2009, 39: 569
- [38] Heravi M M, Bakhtiari K, Oskooie H A, Taheri S. *Heteroat Chem*, 2008, 19: 218
- [39] Khaksar S, Rostamnezhad F. *Bull Korean Chem Soc*, 2012, 33: 2581
- [40] Huang T K, Wang R, Shi L, Lu X X. *Catal Commun*, 2008, 9: 1143
- [41] Ahmad S, Ali M. *Chin J Chem*, 2007, 25: 818
- [42] Darabi H R, Mohandessi S, Aghapoor K, Mohsenzadeh F. *Catal Commun*, 2007, 8: 389
- [43] Go A, Lee G, Kim J, Bae S, Lee B M, Kim B H. *Tetrahedron*, 2015, 71: 1215